11th World Congress on Computational Mechanics (WCCM XI)
5th European Conference on Computational Mechanics (ECCM V)
6th European Conference on Computational Fluid Dynamics (ECFD VI)
E. Oñate, J. Oliver and A. Huerta (Eds)

ANALYSIS AND OPTIMIZATION OF A LIQUID LEAD-BISMUTH TARGET FOR ISOL FACILITIES

DONALD D. HOUNGBO*†, JAN VIERENDEELS* AND LUCIA POPESCU†

* Department of Flow, Heat and Combustion Mechanics
Universiteit Gent (Ugent)
St.-Pietersnieuwstraat 41, B-9000 Gent, Belgium
e-mail: donald.houngbo@ugent.be, jan.vierendeels@ugent.be, www.ugent.be

† Belgian Nuclear Research Centre (SCK•CEN)
Boeretang 200, B-2400 Mol, Belgium
email: lpopescu@sckcen.be, www.sckcen.be

Key Words: *ISOL, Liquid-metal flow, Compact geometry, Design optimization, Recirculation.*

Abstract. In the context of new-generation ISOL facilities, liquid-metal loop targets are proposed to deal with the high driver-beam power on target. In this framework, the circulating liquid Lead Bismuth Eutectic (LBE) target is of interest for high-power facilities like ISOL@MYRRHA[1] [1] and EURISOL[2][2]. When developing this proof-of-concept target, one of the important challenges is to design the shape of the irradiation container so that, once irradiated, the LBE is immediately evacuated into a shower of very small droplets. This is necessary in order to enhance the diffusion of isotopes formed during irradiation, especially important for isotopes with short half-lives.

This study deals with the optimization of the flow of a heavy liquid metal in a compact and complex geometry. The full target geometry and its dimensions have been set as design variables.

Three-dimensional (3-D) computer simulations of the LBE flow have been used for the evaluation of design modifications. Starting from the initial design, the flow features in the target geometry as well as the evolution of these features with the design changes have been computed with the CFD tool FLUENT (Ansys Inc.) [3]. At each step of the target optimization, insight was gained into the influence of different parameters on the flow features. Different improved target geometries were eventually obtained. Each of them showcases a different way to deal with the jet effect initially observed due to the high-momentum inlet liquid stream. Full-scale prototyping and testing of the optimized geometries is ongoing (February 2014).

[1] http://isolmyrrha.sckcen.be/
[2] http://www.eurisol.org/site02/index.php

1 INTRODUCTION

Applications of Radioactive Ion Beams (RIBs) are found in several fields of science, among which nuclear physics, fundamental interactions, nuclear astrophysics [4]... Because of their short half-lives, the only way to produce beams of exotic nuclei is using on-line methods: either in-flight separation (IFS), or the isotope separation on-line (ISOL) [4]. For RIBs of exotic nuclei, the main advantage of the ISOL technique comes from the higher achievable purities, since the study of exotic nuclei is often hindered by the fact that they are submerged in the high background of more stable nuclei also produced in the target. However, it should be noted that decay losses during the isotope-release, ionization and transport processes are an important drawback for the production of very-short lived isotopes (half-lives in the millisecond range).

Worldwide efforts are currently devoted to prepare the new generation of RIB facilities, with the aim of improving by orders of magnitude their general performance compared to presently running facilities. High-power targets development is a major part of this preparation. Different concepts of high-power solid targets have been proposed and studied. However, the primary-beam power at which these targets can be operated is still limited to several tens of kW [5-7]. Moreover, these solid targets are characterized by relatively low thickness in order to radiatively dissipate high power deposition.

An alternative approach is the recently-proposed liquid-metal-loop target [8], which is expected to handle much higher primary-beam power because the target material flows in a loop equipped with a heat exchanger. Additionally, liquid targets offer the highest thickness of any material (~200 g/cm2 for Lead Bismuth Eutectic - LBE).Concerns for the design of these targets include effects such as pressure drop, cavitation, liquid-metal recirculation, instabilities, non-uniform flows etc…[9-11] Studies conducted in the past highlight the importance of these effects on the target system[12, 13].

The study reported here aims at providing solutions to specific hydrodynamics issues of concern for the design of this high-power liquid-metal-loop target. The target design optimization based on criteria detailed in section 2 is also presented, followed by presentation and discussion of different improved concepts.

2 THE CONCEPT OF A LIQUID-METAL-LOOP TARGET

Molten-lead targets have been studied and operated at ISOLDE with 600-MeV protons from the Synchrocyclotron (SC) and later on with 1- to 1.4-GeV protons from the Proton-Synchrotron-Booster (PS-Booster) [14]. These targets were 20-cm long cylinders with a 1-cm radius, partially filled with molten lead. With these targets, the time necessary to release half of the isotopes (T_{50}) from the molten-metal target ranged from 30 - 120 s (SC) to 10 ± 5 s at PS-Booster [15]. Important decay losses are therefore suffered when trying to produce RIBs of short-lived isotopes like ^{178}Hg ($T_{1/2}$ = 0.26 s) and ^{177}Hg ($T_{1/2}$ = 0.17 s).

In order to achieve higher release efficiencies, especially important for short-lived isotopes in the current liquid-metal-loop target, the liquid metal is spread into a shower of small droplets immediately after irradiation (see fig 1). We aimed here at a complete evacuation of the irradiated LBE from the irradiation volume within 100 ms after a proton pulse impact.

The characteristic diffusion length of isotopes is reduced in the present concept by decreasing the size of the LBE matrix out of which nuclides have to diffuse. The formation of

droplets with radii in the range of a few 100 µm represents a decrease in the characteristic diffusion length of isotopes of two orders of magnitude compared to previous ISOLDE molten-lead targets.

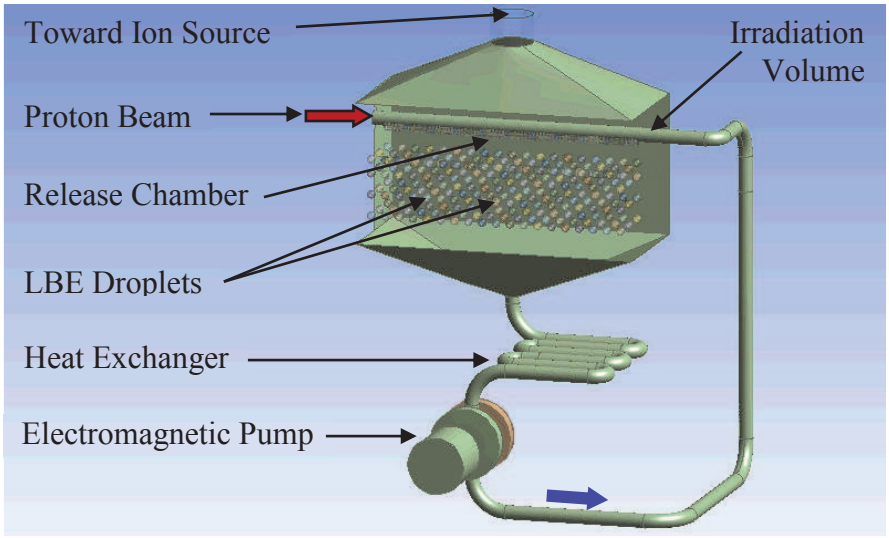

Figure 1: Conceptual view of the liquid-LBE-loop target

Each of the small droplets constitutes the matrix out of which the isotopes will diffuse. The shape of the droplets also influences the characteristic diffusion length of isotopes, and the sphere is the ideal shape for fast release [8, 16]. Therefore, the present target aims at producing spherical LBE droplets. Applying the Young-Laplace law [17], we derived that spherical droplets of LBE will be produced provided the following condition is met :

$$r \ll \sqrt{\frac{\gamma}{g\left(\rho_{liq}-\rho_{vap}\right)}} \tag{1}$$

where r is the spherical-droplet radius, γ is the surface tension of LBE, ρ_{liq} and ρ_{vap} are the respective densities of liquid and vapor LBE, while g is the gravity. At the pressure of the release chamber (p ~5 10^{-7} mbar), the produced droplets will be spherical if their radii are much smaller than 2 mm. This condition is met for 200-µm radii droplets, with a 1% maximum deviation of the droplet-surface mean curvature from the ideal spherical curvature.

LBE droplets form a shower inside the release chamber of the target as illustrated by fig 1. They fall under gravity before being collected at the bottom of the release chamber and, meanwhile, isotopes diffuse out of these droplets to effuse towards the ion source via the transfer tube. The heat exchanger is foreseen upstream to the pump to insure that the LBE temperature at the pump inlet does not exceed maximum acceptable values for the magnets of the pump (~600 °C). This layout can be afforded since the electromagnetic pump foreseen is not prone to cavitation. However, the design needs to ensure that the hydrostatic pressure build-up below the release chamber is sufficient to compensate for the pressure drop in the heat exchanger.

3 METHODOLOGY

Computational Fluid Dynamics (CFD) tools are commonly utilized for the thermal and hydraulic design of facilities operating with liquid-metal [10, 18, 19]. Furthermore, CFD analysis has been validated in the framework of thermal-hydraulics design of the MEGAPIE LBE target [10, 20]. Indeed, the experimental validation of the optimized design of this target has confirmed CFD prediction of important points such as the turbulence modeling, pressure field and pressure drop in a liquid-metal flow. Because these tools are less expensive and faster to implement for a design optimization procedure than prototyping each optimization step, a commercial CFD tool, Fluent (ANSYS, Inc.), has been used for the work reported in this article. Full-scale prototyping and tests following the design study are currently underway to validate CFD calculations.

All the modeled CFD geometries comprise a half-symmetry of the target geometry about the vertical plane at z=0 on fig 2 (see fig 5 for some half-symmetry views). This assumption is explained by the fact that the distributions of evacuation and feeder apertures are symmetric with respect to the vertical mid-plane of the flow inlet. The geometries were also restricted to the fluid domain for CFD analysis and the fluid-container interaction has been modeled by adequate “no slip wall” boundary conditions. About fifteen million cells are required to get mesh-independent results in the half-symmetry distributed-inlet concepts. The thermal effects of the proton-beam impact have not been taken into account in these calculations. This simplifies and speeds-up calculations during the hydro-dynamical optimization process. Issues related to LBE temperature profile, heat deposition and dissipation, potential occurrence of pressure waves and resonance are treated at a later stage.

Previous liquid-metal target design calculations with k-ϵ and k-ω Shear Stress Transport (SST) turbulence models have shown good agreement with experimental data for average-flow behavior and mean-velocity fields [21, 22]. Because these models are less computational expensive and since no energy-mixing process is accounted for in this design-optimization process, the SST k-ω turbulence model has been used for these steady-state simulations. In practice, the steady-state LBE flow would be disturbed by the energy deposition from the highly-pulsed beam. However, previous calculations with the ISOLDE [23] proton-beam conditions indicate that the flow perturbation and thus the deviation from steady-state flow should only last for fractions of ms after a proton-pulse impact [11]. This, in association with the fact that thermal effects of the proton-beam impact are not accounted for at this stage, explains the use of steady-state simulations.

One major objective mentioned earlier is that of evacuating all the irradiated LBE from the irradiation volume within 100 ms after a proton pulse. In order to check if this condition was met, transient simulations were run with the steady-state results as initial conditions. In these transient simulations, we have monitored over time the inflow of non-irradiated LBE in the irradiation volume. Thus, the rate of evacuation of the irradiated LBE from the different concepts after 100 ms was determined. Since as explained in the previous paragraph, flow perturbations resulting from the energy deposition of the proton pulse are not expected to sustain for a long period of time, this effect has not been considered either in the transient calculations.

4 STARTING-CASE GEOMETRIES OF THE TARGET CONTAINER

4.1 Concept

Based on the conceptual view presented on fig 1, the starting-case geometry presented on fig 2 (left) was used for LBE dynamics simulation inside the target container. In this concept, the target container consists of a 20-cm long and 1-cm diameter cylinder. This diameter is selected to accommodate three standard deviations (3σ) of the proton-beam transverse Gaussian profile. The cylindrical container and proton-beam direction (red arrow on fig 2) are coaxial and, LBE flows into the target container through its base section (blue arrow on fig 2) and flows out through the lower half of its lateral surface.

Concept 1 features 2500 evacuation apertures of 200-µm radii, numbers deriving from the objectives of having 100-ms fast evacuation and reaching the proper regime of droplet formation (the jetting regime [24]).

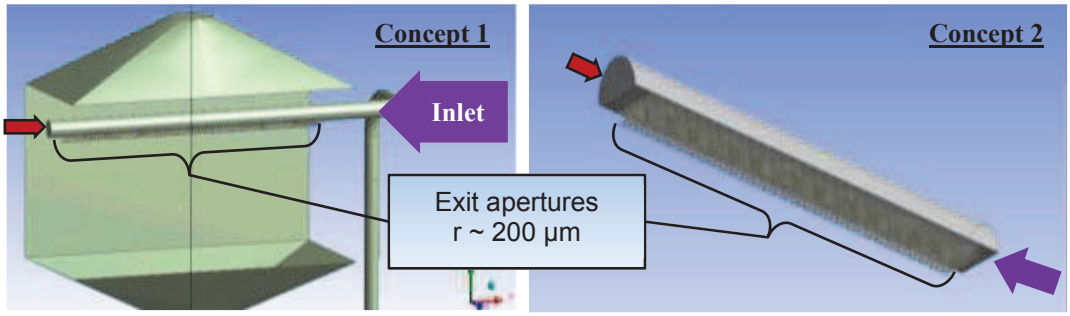

Figure 2: Target container starting-case geometries : full cylindrical concept 1 with exit apertures on lower half of lateral surface and half-cylindrical concept 2 with exit apertures on the flat base surface

Considering the fact that the manufacturing of the exit apertures on a cylindrical surface is quite challenging, an alternative concept featuring the evacuation apertures on a flat surface (see fig 2, right) was also initially considered. The geometry of concept 2 consists of the half of a 2-cm diameter cylinder in order to accommodate 3σ for the proton beam. The cross-section area and flow rate of the target container in concept 2 are correspondingly twice the values in concept 1. Because the flow rate is doubled, 5000 evacuation apertures are required in Concept 2, in order to keep the formation of droplets in the same regime.

4.2 Results & discussion

The static-pressure distributions of concept 1 and concept 2 (fig 3, a & b), show very low pressure levels in the LBE inside the evacuation apertures on the inlet side of the irradiation volume. Some of these low-pressure cells have pressure values below experimental values of the LBE saturation vapor pressure reported in literature [9, 25] at 500 K, 10^{-6} Pa. This poses risks of cavitation. Evidence of typical corrosion pattern caused by cavitation have been reported for ISOLDE molten-metal target containers [26]. In addition, cavitation is a greater concern for high-power targets, mainly due to the higher intensity of the primary beam. Therefore, cavitation risks are to be avoided in this target design, since it is detrimental for the target container life time, and can even lead to failure of the latter.

The low pressure zones in fig 3 are explained by the fact that high-pressure gradients are

required to bend the high-momentum LBE streamlines through the first apertures on the inlet side. The low-pressure values computed inside the irradiation volume at the inlet side were low enough to induce virtually no flow through the corresponding evacuation apertures, which also means no droplet formation through these apertures.

Pressure progressively builds up inside the irradiation chamber in both concepts 1 and 2 while the average horizontal velocity decreases (from right to left on fig 3). This is due to the fact that part of the inlet LBE flow is progressively lost through the evacuation apertures leading to a lower flow rate while the cross section of the flow volume is constant along the irradiation volume.

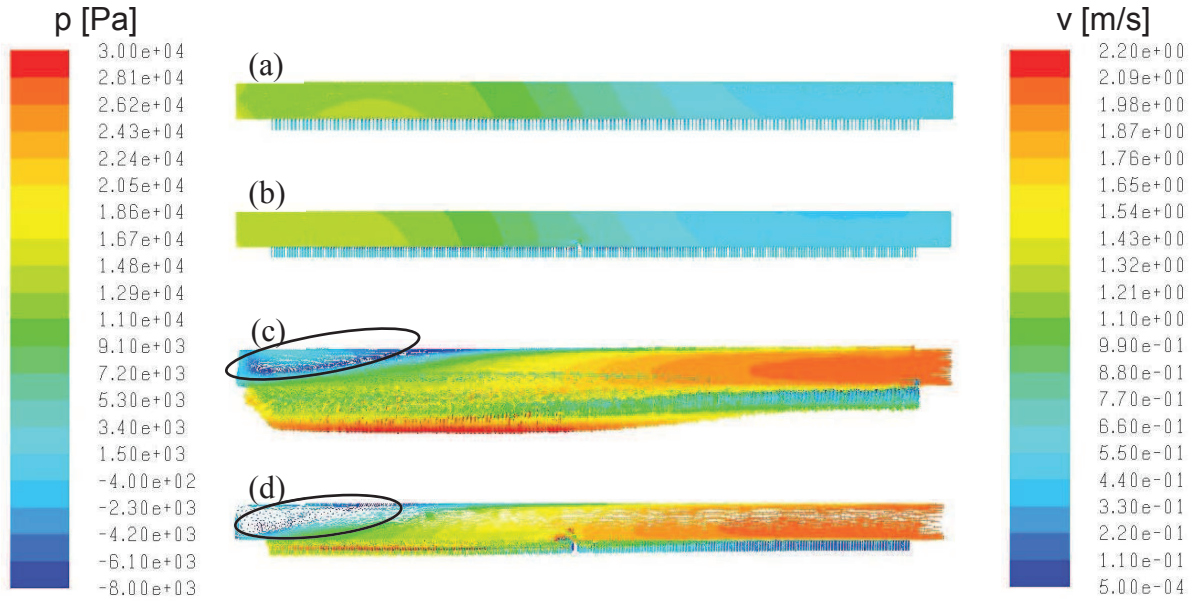

Figure 3: Static-pressure contours of (a) concept 1 & (b) concept 2, Velocity vectors for (c) concept 1 & (d) concept 2 (note that LBE flows in from right to left)

The negative values on the pressure scales are not only related to the high-momentum streamline bending effect described earlier. Because of the stream-wise pressure build-up mentioned in the previous paragraph, an acceleration of LBE at the entrance in evacuation apertures mostly on the left-hand side of the plots on fig 3 leads as well to computation of negative pressure values in the corresponding cells. Computation of these, however, unphysical negative pressure values occurs because cavitation effects were not modeled. Modeling these effects is not needed at this stage and would increase computation time.

Recirculation zones were also noticed at stream-wise end of the irradiation volume in both concepts (circled in black on fig 3) because of the direction change and the reduced momentum of the flow. When they occur in the irradiation volume, these recirculation zones carry produced isotopes for extended periods of time and therefore lead to significant decay-losses of short-lived isotopes that are not promptly evacuated in the release chamber. Recirculation zones inside the irradiation zone may additionally lead to creation of hot spots.

The effect of recirculation zones was studied by analysing the portion of irradiated LBE evacuated from the irradiation volume at 100 ms after the arrival of a proton pulse. The irradiated LBE is labelled with the yellow color while the non-irradiated LBE is colored in red (fig 4 & 7). It is shown on fig 4 that after 100 ms following the arrival of a proton pulse, portions of irradiated LBE in the recirculation zones have not been evacuated from the irradiation volume to the release chamber. Recirculation zones in the irradiation volume are therefore to be avoided.

Figure 4: Refreshment state of irradiated LBE (yellow) in (a) concept 1 and (b) concept 2 100 ms after arrival of a proton pulse. Red color represents non-irradiated LBE.

In summary, issues detected for concepts 1 and 2 are the presence of very low pressure zones, a non-uniform distribution of evacuation velocity vectors along the proton beam direction and LBE recirculation inside the irradiation volume. Consequently, these simple concepts cannot be used. Therefore, the target-container design-optimization presented in the following lines considered successively-improved concepts to overcome these issues.

From this point on, the half-cylinder design of the target-container in concept 2 has been dropped because of three major disadvantages:

- larger irradiation chamber volume,
- higher flow rate i.e. it requires more power at the pump (pressure drops being of the same order as in concept 1),
- more evacuation apertures per unit surface, meaning higher cost for manufacturing and higher risks of merging between closer LBE jets.

Different improved concepts are presented and analyzed in the following sections.

5 IMPROVED TARGET CONTAINERS

5.1 Concept

The different target-container concepts presented from this point on feature LBE inlets that are perpendicular to the proton-beam axis. This transverse arrangement of inlets was set in order to avoid the necessary bending of high-momentum streamlines over the evacuation apertures close to the coaxial inlet as we have noticed for concepts 1 and 2. As a result, the issue of low-pressure spots observed close to the inlet in concept 1 and concept 2 was solved. The inlet velocities are adapted to the available inlet cross-section in each different concept in order to compare them based on the same flow rate.

Specific to these concepts is the insertion of a feeder volume and feeder grids between the inlet and the irradiation volume. In combination, the feeder volume and feeder grids are used to oppose some inertial and viscous resistance to the inlet jet, thus distributing it over the irradiation volume. Besides, by straightening the direction of velocity vectors inside the irradiation volume and making them normal to the proton-beam axis, the feeder volume and feeder grid combination is useful to prevent occurrence of recirculation inside the irradiation volume. This concept is further improved through the use of a large feeder volume.

By increasing the area of the feeder-volume cross section (normal to the direction of the beam on fig 5), the mean horizontal velocity of LBE inside the feeder volume is reduced. This decreases the friction effects on LBE flowing along the feeder grid and results in a uniform distribution of the LBE velocity through uniformly-distributed feeder-grid apertures (see fig 6, c & d). Figure 5 presents the geometry of two different large feeder volume concepts used to meet the dual objective of a uniform distribution of evacuation velocities as well as vertical orientation of velocity vectors inside the irradiation volume.

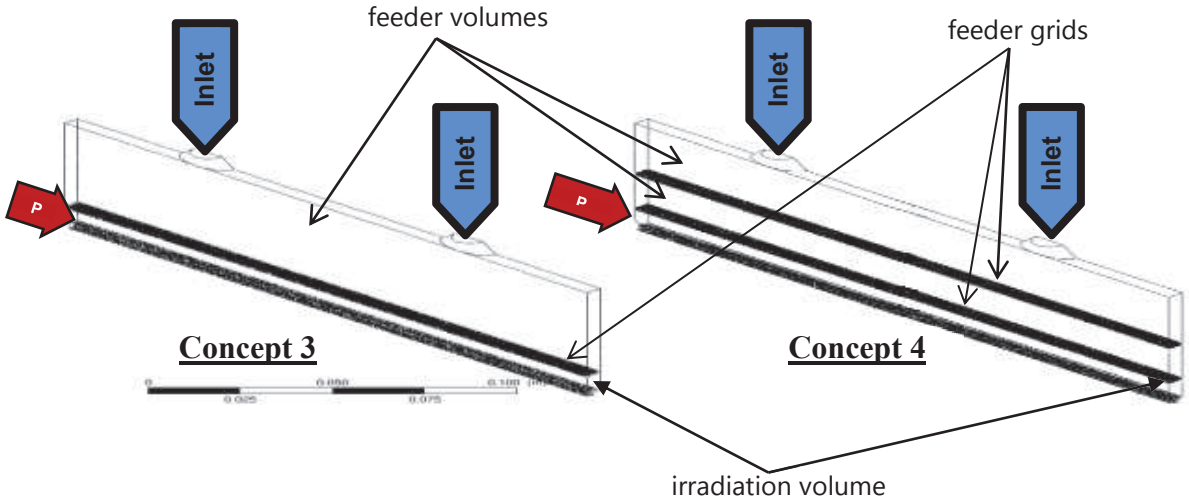

Figure 5: Half-symmetry view of large feeder volume target containers (concepts 3 & 4)

In concept 3, smaller feeder-grid apertures (100-µm radii) were required in order to oppose sufficient resistance to the inlet jets and to get a uniform LBE flow through the irradiation volume. In concept 4, a second identical feeder grid was necessary to meet the same goal with 200-µm radii feeder-grid apertures.

5.2 Results & discussion

As shown on the plots of velocity vectors (fig 6, c & d), the feeder grids distribute the inlet jet flow over the irradiation volume, thereby leading to a more uniform distribution of evacuation-velocity vectors at the outlet of the irradiation volume. With a feeder volume sufficiently large that reduces friction on the LBE flow along the feeder grid, mostly constant pressure differences are obtained vertically across the grids (fig 6, a & b), explaining the uniformity of velocity-vectors distribution inside the irradiation chamber and at evacuation.

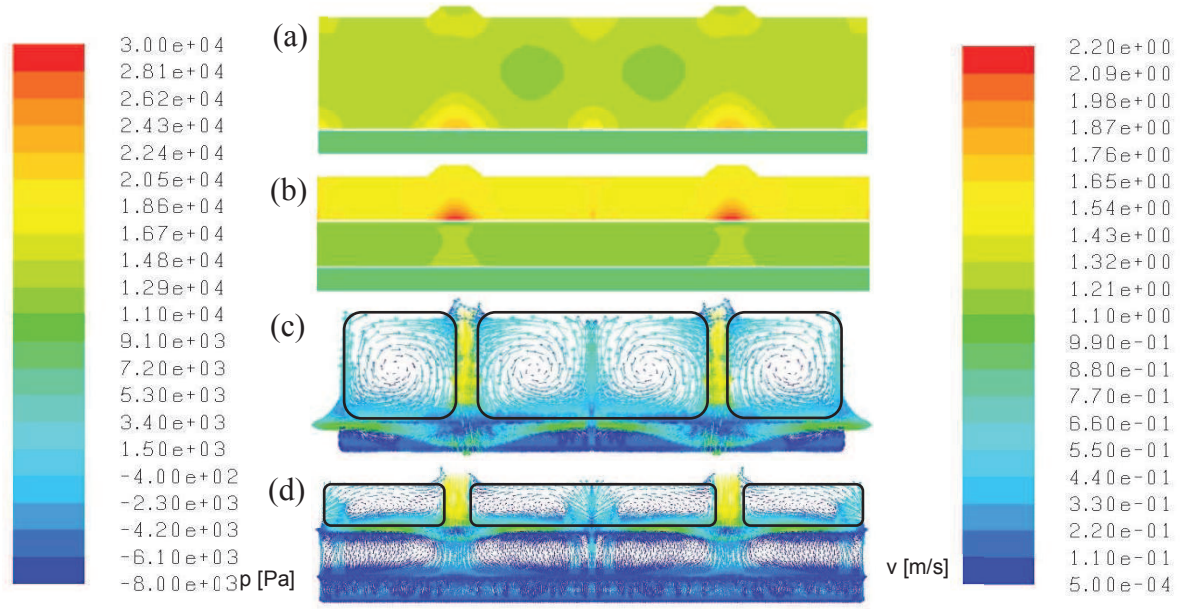

Figure 6: Static-pressure contours of (a) concept 3 & (b) concept 4, Velocity vectors for (c) concept 3 & (d) concept 4, recieculation zones (in black boxes) occur out of the irradiation volumes.

The feeder grids also have the effect of straightening the flow, ensuring that velocity-vectors inside the irradiation chamber are normal to the beam axis, suppressing the recirculation zones inside the irradiation chamber. Recirculation zones are only noticed in the feeder volume (see black rounded rectangles on fig 6, c & d). As a result, in both concepts 3 and 4, all the irradiated LBE (yellow) has been evacuated from the irradiation chamber, 100 ms after proton-pulse impact (see fig 7).

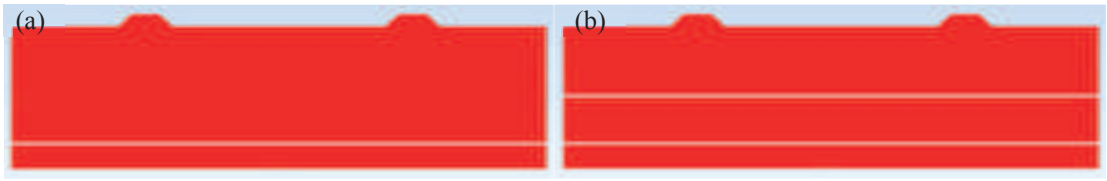

Figure 7: Refreshment state of the LBE at 100 ms after the proton pulse in (a) concept 3, (b) concept 4. The LBE irradiated by this proton pulse would be fully evacuated and only non- irradiated LBE (red color) is present in the irradiation volume for both concepts.

7 CONCLUSIONS

The CFD simulations presented here have been carried out in support of the design and optimization process of a molten-LBE target loop for the production of beams of short-lived radioactive ions at high-power ISOL facilities. CFD analysis was used since it has been validated in the past with experimental data for LBE. It also allowed us to avoid a lengthy and

costly process of prototyping and testing every investigated design.

The target-design optimization reported here was conducted with the aim of fully evacuating the irradiated LBE from the irradiation volume within 100 ms after the impact of a proton pulse. Two alternative designs meeting this requirement have been presented. In each of these cases the inlet-jet effect was dealt with via a combination of two approaches: (1) using two inlets in order to increase the total inlet section and reduce inlet velocities, and (2) opposing one or two high-resistance feeder grids to the inlet jet.

With this strategy, within a compact geometry, the high-momentum inlet-jet flow is transformed into a uniform flow in the irradiation volume and at evacuation apertures. Low-pressure zone issues have been solved by avoiding unnecessary bending of the flow inside the compact geometry of the target. In addition, the ideal spherical shape of the LBE droplets is ensured by making small droplets (radii << 2 mm).

The satisfactory concepts are being prototyped within the LIEBE[3] project and will be tested for validation of the computed flow pattern against experimental data. Tests are scheduled at CERN-ISOLDE.

ACKNOWLEDGEMENTS

This work was supported by the Belgian Science Policy Office through the IAP programme (BriX network P6/23), We acknowledge discussions with the LIEBE collaboration partners.

REFERENCES

[1] Popescu L. Nuclear-physics applications of MYRRHA. (*in print*) accepted for publication in EPJ Web of Conferences (2014), issue on the 25th International Nuclear Physics Conference. Firenze, Italy; June 2-7, 2013.

[2] Blumenfeld Y, Butler P, Cornell J, Fortuna G, Lindroos M. EURISOL DESIGN STUDY: TOWARDS AN ULTIMATE ISOL FACILITY FOR EUROPE. International Journal of Modern Physics E-Nuclear Physics 2009;18(10):1960-4.

[3] ANSYS I. ANSYS FLUENT Theory Guide. Southpointe
275 Technology Drive
Canonsburg, PA 15317; November 2011.

[4] Huyse M. The Why and Howof Radioactive-Beam Research. In: Al-Khalili J, Roeckl E, editors. The Euroschool Lectures on Physics with Exotic Beams, Vol I: Springer Berlin Heidelberg; 2004. p. 1-32.

[5] Y. Zhang GDA. Design of high-power ISOL targets for radioactive ion beam generation. Nuclear Instruments and Methods in Physics Research Section A: Accelerators, Spectrometers, Detectors and Associated Equipment 2004;521(1):72–107.

[6] M. Dombsky PB. High intensity targets for ISOL, historical and practical perspectives. Nuclear Instruments and Methods in Physics Research Section B: Beam Interactions with Materials and Atoms 2008;266(Issues 19–20):4240–6.

[7] Bricault P, Dombsky M, Dowling A, Lane M. High power target developments at ISAC. Nuclear Instruments & Methods in Physics Research Section B-Beam Interactions with Materials and Atoms 2003;204:319-24.

[8] Board EpC. Final report of the EURISOL design study (2005-2009). Cornell, John C edn: GANIL; 2009. p. 220.

[3] LIquid lEad Bismuth eutectic Experiment (LIEBE) project

[9] Dury TV. CFD design support at PSI for the international MEGAPIE liquid-metal spallation target. Journal of Nuclear Science and Technology 2004;41(3):285-95.
[10] Samec K, Milenković RŽ, Dementjevs S, Ashrafi-Nik M, Kalt A. Design of a compact high-power neutron source—The EURISOL converter target. Nuclear Instruments and Methods in Physics Research Section A: Accelerators, Spectrometers, Detectors and Associated Equipment 2009;606(3):281-90.
[11] Noah E, Bruno L, Catherall R, Lettry J, Stora T. Hydrodynamics of ISOLDE liquid metal targets. Nuclear Instruments & Methods in Physics Research Section B-Beam Interactions with Materials and Atoms 2008;266(19-20):4303-7.
[12] Milenković RŽ, Dementjevs S, Samec K, Flerov A, Thomsen K. Wavelet analysis of experimental results for coupled structural–hydraulic behavior of the EURISOL target mock-up. Nuclear Instruments and Methods in Physics Research Section A: Accelerators, Spectrometers, Detectors and Associated Equipment 2009;608(1):175-82.
[13] Jung P, Koppitz T, Muller G, Weisenburger A, Futakawa M, Ikeda Y. Improved cavitation resistance of structural materials in pulsed liquid metal targets by surface hardening. Journal of Nuclear Materials 2005;343(1-3):92-100.
[14] Lettry J, Catherall R, Drumm P, Van Duppen P, Evensen AHM, Focker GJ, et al. Pulse shape of the ISOLDE radioactive ion beams. Nuclear Instruments and Methods in Physics Research Section B: Beam Interactions with Materials and Atoms 1997;126(1–4):130-4.
[15] Lettry J, Catherall R, Cyvoct G, Drumm P, Evensen AHM, Lindroos M, et al. Release from ISOLDE molten metal targets under pulsed proton beam conditions. Nuclear Instruments & Methods in Physics Research Section B-Beam Interactions with Materials and Atoms 1997;126(1-4):170-5.
[16] Fujioka M, Arai Y. Diffusion of radioisotopes from solids in the form of foils, fibers and particles. Nuclear Instruments and Methods in Physics Research 1981;186(1–2):409-12.
[17] Lautrup B. Physics of Continuous Matter, Second Edition: Exotic and Everyday Phenomena in the Macroscopic World: Taylor & Francis; 2011.
[18] Vanderhaegen M, Vierendeels J, Arien B. CFD analysis of the MYRRHA primary cooling system. Nuclear Engineering and Design 2011;241(3):775-84.
[19] Wolters J, Hansen G, J. KEM, F. R. Validation of CFD Models with Respect to the Thermal-Hydraulic Design of the ESS target. IAEA Technical Meeting. Karlsruhe, Germany; 2003.
[20] Fazio C, Gröschel F, Wagner W, Thomsen K, Smith BL, Stieglitz R, et al. The MEGAPIE-TEST project: Supporting research and lessons learned in first-of-a-kind spallation target technology. Nuclear Engineering and Design 2008;238(6):1471-95.
[21] Samec K, Milenkovic RZ, Blumenfeld L, Dementjevs S, Kharoua C, Kadi Y. Measurement and analysis of turbulent liquid metal flow in a high-power spallation neutron source-EURISOL. Nuclear Instruments & Methods in Physics Research Section a-Accelerators Spectrometers Detectors and Associated Equipment 2011;638(1):1-10.
[22] Stieglitz R, Daubner M, Batta A, Lefhalm CH. Turbulent heat mixing of a heavy liquid metal flow in the MEGAPIE target geometry—The heated jet experiment. Nuclear Engineering and Design 2007;237(15–17):1765-85.
[23] Kugler E. The ISOLDE facility. Hyperfine Interactions 2000;129(1-4):23-42.
[24] Clanet C, Lasheras JC. Transition from dripping to jetting. Journal of Fluid Mechanics 1999;383:307-26.
[25] Agency NE. Handbook on Lead-bismuth Eutectic Alloy and Lead Properties, Materials Compatibility, Thermal-hydraulics and Technologies. In: OECD, editor.; 2007.
[26] Lettry J, Arnau G, Benedikt M, Gilardoni S, Catherall R, Georg U, et al. Effects of thermal shocks on the release of radioisotopes and on molten metal target vessels. Nuclear Instruments and Methods in Physics Research Section B: Beam Interactions with Materials and Atoms 2003;204(0):251-6.